

Cite this: *J. Mater. Chem. C*, 2020,  
8, 9352Received 18th December 2019,  
Accepted 18th May 2020

DOI: 10.1039/c9tc06919d

rsc.li/materials-c

## Defect compensation in the p-type transparent oxide $\text{Ba}_2\text{BiTaO}_6$ †

Diana Dahliah,<sup>†</sup> Gian-Marco Rignanese<sup>†</sup> and Geoffroy Hautier<sup>†\*</sup>

$\text{Ba}_2\text{BiTaO}_6$  is a transparent p-type oxide recently discovered and exhibiting attractive hole mobility but low carrier concentration. Using first-principles computations, we study how defects influence the carrier concentration in  $\text{Ba}_2\text{BiTaO}_6$ . The calculated defect formation energies confirm that K is an adequate p-type shallow extrinsic dopant but that high p-type doping is prevented by the presence of compensating, “hole-killing”, intrinsic defects: O vacancies but also Ta on Bi anti-sites. Our work stresses the inherent difficulty in doping  $\text{Ba}_2\text{BiTaO}_6$  to high carrier concentration and discusses a few avenues towards this goal.

### Introduction

Transparent conducting oxides (TCOs) simultaneously display transparency to visible light and good electrical conductivity. Such an unusual combination of properties can be achieved by doping (n-type or p-type) a wide band-gap material.<sup>1–3</sup> TCOs have received much attention in the last decades due to their critical role in various industrial applications from touch screens to solar cells and light emitting devices.<sup>3–7</sup> Various high-performance n-type TCOs (such as Sn-doped  $\text{In}_2\text{O}_3$ ,<sup>4</sup> Al-doped  $\text{ZnO}$ ,<sup>8,9</sup> or F-doped  $\text{SnO}_2$ <sup>10–12</sup>) have been developed and are widely used industrially. In contrast, p-type TCOs are still lagging behind in part because of their rather poor carrier mobility. Indeed, while most oxides have highly dispersive conduction bands leading to low electron effective mass in n-type TCOs, the O-2p nature of the top of their valence bands induces rather flat bands, and hence high effective mass and low hole mobility.<sup>3,13,14</sup> Filling the gap in properties between n- and p-type TCOs would contribute to breakthroughs in transparent electronics or new thin film solar cell design. Kawazoe *et al.*<sup>15</sup> found that, in  $\text{CuAlO}_2$ , the curvature of the valence band is increased due to the mixing of the O-2p orbitals with the 3d-orbitals of Cu cations, hence lowering their effective mass.<sup>15</sup> This work generated extensive investigation in the field of Cu-based p-type TCOs<sup>3,15</sup> followed by exploration of other chemistries for instance targeting 5s-based cations such

as  $\text{Sn}^{2+}$ ,<sup>10,11,16,17</sup> or mixed anionic materials.<sup>18–21</sup> In this quest for new p-type TCOs, high-throughput computational screening has been used recently to identify interesting materials candidates.<sup>13,22</sup> Among these, the double perovskite  $\text{Ba}_2\text{BiTaO}_6$  showed very promising properties combining a wide band gap, low hole effective mass (hence, high hole mobility) and a valence band high enough in energy to expect p-type behavior.<sup>23</sup> The low hole effective mass in this perovskite can be attributed to the mixing of the Bi-6s and O-2p orbitals gives rise to a strong delocalization at the top of the valence band. This behavior of Bi-6s is quite unique to  $\text{Ba}_2\text{BiTaO}_6$  as previous attempts to use  $\text{Bi}^{3+}$  to obtain a mixing with O-2p orbitals failed as the Bi-6s orbitals were too low in energy.<sup>24</sup> Experimental synthesis and characterization of  $\text{Ba}_2\text{BiTaO}_6$  confirmed its transparency and a remarkable hole mobility of  $30 \text{ cm}^2 \text{ V}^{-1} \text{ s}^{-1}$  after K doping.<sup>23</sup> Unfortunately, only very limited hole carrier concentrations ( $10^{14} \text{ cm}^{-3}$ ) could be achieved experimentally, resulting in low conductivity. This low hole carrier concentration despite an important presence of dopants indicates that defects compensation mechanisms are likely to be at play.

Here, we use first-principles computations to study the defect chemistry in  $\text{Ba}_2\text{BiTaO}_6$  to shed light on the factors limiting its dopability. We identify the compensating defects responsible for the poor doping performances of the material and suggest avenues to improve carrier concentrations in  $\text{Ba}_2\text{BiTaO}_6$ .

### Methods

All calculations were performed using Density Functional Theory (DFT) adopting the Projector Augmented Wave (PAW) method<sup>25</sup> as implemented in the Vienna Ab initio Simulation Package (VASP).<sup>26,27</sup> The wavefunctions were expanded on a plane-wave basis set employing a cutoff energy of 520 eV. The point defects were studied using

*Institute of Condensed Matter and Nanoscience, Université catholique de Louvain, Cheminétoiles 8, bte L7.03.01, Louvain-la-Neuve 1348, Belgium.*

*E-mail: geoffroy.hautier@uclouvain.be*

† Electronic supplementary information (ESI) available: The lattice parameters and bond lengths of  $\text{Ba}_2\text{BiTaO}_6$  calculated within PBE and HSE, the point defects formation energies in  $\text{Ba}_2\text{BiTaO}_6$  and  $\text{Ba}_2\text{BiSbO}_6$  computed within PBE, as well as the PBE band structure of  $\text{Ba}_2\text{Bi}_{1.125}\text{Ta}_{0.875}\text{O}_6$ . The CIF files of all relaxed super-cells with each functional are also provided. See DOI: 10.1039/c9tc06919d

the supercell approach.<sup>28</sup> The different atomic models were generated using the Python Charge Defects Toolkit (PyCDT)<sup>29</sup> starting from a supercell with 128 atoms. The Brillouin zone was sampled using a  $\Gamma$  only  $k$ -point grid. The exchange–correlation (XC) potential was first obtained through the generalized gradient approximation using the Perdew–Burke–Ernzerhof (PBE) functional.<sup>30</sup> Then, for the defects with the lowest PBE formation energy, new calculations (including structural relaxation) were performed adopting the Heyd–Scuseria–Ernzerhof (HSE) hybrid functional with an exact-exchange fraction of 0.25 and a screening length of 0.2 Å.<sup>31,32</sup> More details about the lattice constants and bond lengths for the two XC functionals employed are given in ESI.† All the models were relaxed at fixed volume (spin-polarized calculations were performed) till the maximum force on the ions became smaller than 0.1 eV Å<sup>-1</sup>. The occupation of the electronic states was determined through the Gaussian smearing method with a smearing width of 0.05 eV. The formation energy of each charged defect state was computed as a function of the Fermi level  $E_f$  as:<sup>33,34</sup>

$$E_{\text{form}}[X^q] = E_{\text{tot}}[X^q] - E_{\text{tot}}^{\text{bulk}} - \sum n_i \mu_i + qE_f + E_{\text{corr}} \quad (1)$$

where  $E_{\text{tot}}[X^q]$  and  $E_{\text{tot}}^{\text{bulk}}$  are the total energies of the defective supercell (for a given defect  $X$  in the charge state  $q$ ) and the bulk energy respectively. The third term represents the energy needed to exchange atoms with thermodynamic reservoirs where  $n_i$  indicates the number of atoms of the species  $i$  removed or added to create the defect, and  $\mu_i$  are their corresponding chemical potential. The fourth term represents the energy to exchange electrons with the host material through the electronic chemical potential which is the Fermi energy level  $E_f$ . Finally, the last term in the equation is a correction accounting for the finite size of the supercell. Here, we used the extended Freysoldt's (Kumagai's) scheme.<sup>35,36</sup> The equilibrium Fermi level is obtained at a given temperature by imposing charge neutrality and finding a self-consistent solution to the carriers and defects concentrations.

## Results

Fig. 1a shows the double perovskite Ba<sub>2</sub>BiTaO<sub>6</sub> rhombohedral R3 structure. Both Bi<sup>3+</sup> and Ta<sup>5+</sup> are at the center of tilted

octahedra and Ba<sup>2+</sup> fills the larger A site. Fig. 1b shows the band structure of Ba<sub>2</sub>BiTaO<sub>6</sub> computed with HSE. The low hole effective mass is striking with the highly curved valence band. The computed band gap is around 3.6 eV which is close to our previous computations using the GW approximation (3.8 eV).<sup>23</sup> Both values are smaller than the experimental value (4.5 eV).<sup>23</sup> Experimentally, a high hole mobility (30 cm<sup>2</sup> V<sup>-1</sup> s<sup>-1</sup>) indicative of a low hole effective mass was measured through the Hall effect. However, the hole carrier concentration remained small around 10<sup>14</sup> cm<sup>-3</sup> despite an important amount of K added and substituting on the Ba site (as evidenced by a change in the lattice parameter).<sup>23</sup> In order to understand the reasons behind this low carrier concentration, we computed the defects formation energies from first-principles. First all possible charged intrinsic defects, the cation vacancies (Vac<sub>Ba</sub>, Vac<sub>Bi</sub>, Vac<sub>Ta</sub>), the anion vacancy Vac<sub>O</sub>, and the anti-sites of Bi<sub>Ta</sub> and Ta<sub>Bi</sub> as well as the extrinsic K substitutions (K<sub>Ba</sub>, K<sub>Bi</sub>, K<sub>Ta</sub>) were computed within PBE (more details are available in the ESI†). In a second step, the lowest lying defects (Vac<sub>O</sub>: [0, +2], Vac<sub>Ba</sub>: [0, -2], Vac<sub>Bi</sub>: [0, -3], Ta<sub>Bi</sub>: [2, 3], Bi<sub>Ta</sub>: [0, -1, +1] and K<sub>Ba</sub>: [0, -1]) were computed with the more accurate HSE functional. Fig. 2 shows the defect formation energies within HSE as a function of the Fermi level. The formation energies depend on the elemental chemical potential and by studying the competition of Ba<sub>2</sub>BiTaO<sub>6</sub> with other phases, we can set limits to the possible chemical potentials. In Fig. 2 the defect formation energy is reported as a function of the Fermi level for two sets of chemical potential values corresponding to the least (Fig. 2a) and most (Fig. 2b) favorable conditions for p-type doping. The Fermi level can be computed at 300 K by imposing charge neutrality conditions and taking into account the competition between all the defects. This equilibrium Fermi level is shown in dashed orange line for the intrinsic conditions. It is found to be closer to the valence band than to the conduction band in both least and most favorable p-type conditions. However, it remains too far from the VBM to induce a significant amount of carriers. Our defect computations are in agreement with the experimental observation that Ba<sub>2</sub>BiTaO<sub>6</sub> is not intrinsically doped and exhibits negligible conductivity in both pellet and thin film forms.<sup>23</sup> Introducing a shallow defect that is relatively

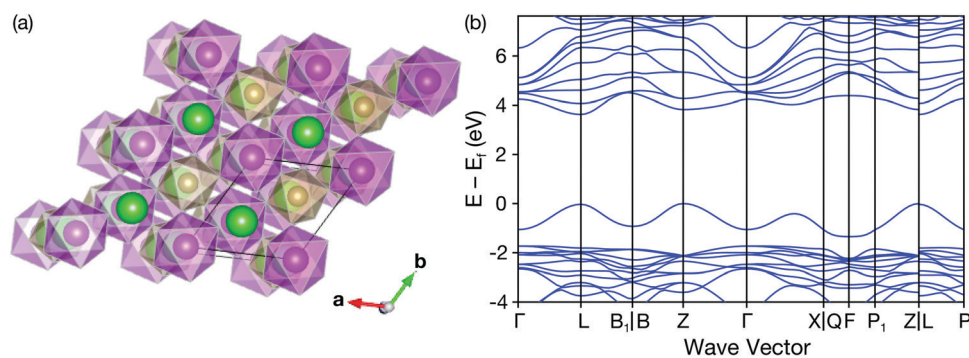


Fig. 1 (a) The crystal structure of a  $2 \times 2 \times 1$  super cell of Ba<sub>2</sub>BiTaO<sub>6</sub> in the rhombohedral R3 structure. The Bi coordination octahedra are represented in purple, while the Ta coordination octahedra are in brown, and the Ba atoms in green, (b) Band structure of Ba<sub>2</sub>BiTaO<sub>6</sub> along high-symmetry lines as computed with HSE.

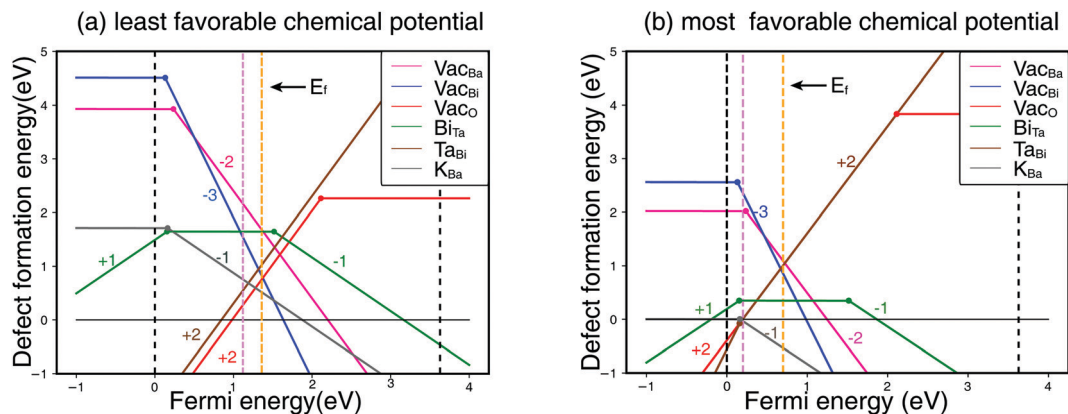


Fig. 2 Defect formation energies as a function of the Fermi energy computed from HSE at the (a) least favorable or (b) most favorable chemical potentials for p-type doping. The dashed orange and purple lines show the Fermi level respectively in the intrinsic and with K-doping conditions.

low in energy such as replacing Ba by K ( $K_{Ba}^{1-}$  in grey) moves the Fermi level closer to the VBM as shown by the purple dashed line. Our results confirm that K is an adequate substitutional defect as we would have guessed from their very similar ionic radii and previous evidences on related compounds such as  $BaBiO_3$ .<sup>37</sup> However, the Fermi level is pinned and cannot approach the VBM closer even in the presence of K doping because of low-lying electron donors such as the O vacancy ( $Vac_O^{2+}$  in red) and the Ta on Bi anti-site defect ( $Ta_{Bi}^{2+}$  in brown). These two defects act as “hole-killers” and prevents the  $E_f$  to move closer to the VBM and to significantly p-type dope  $Ba_2BiTaO_6$ .

Qualitatively our results show that two donors ( $Vac_O^{2+}$  and  $Ta_{Bi}^{2+}$ ) limit the conductivity of the material and act as “hole-killers”. To be more quantitative, we computed the hole concentration in the system at all possible growth conditions. The range of growth conditions is complex with five chemical potentials ( $\mu_{Ba}$ ,  $\mu_{Ta}$ ,  $\mu_{Bi}$ ,  $\mu_O$ , and  $\mu_K$ ) which can take different values. Due to the presence

of the low-lying shallow acceptors ( $K_{Ba}^{1-}$ ) and hole-killers ( $Vac_O^{2+}$  and  $Ta_{Bi}^{2+}$ ), we decided to plot the carrier concentration as a function of  $\mu_K - \mu_{Ba}$  (which sets the amount of K),  $\mu_{Bi} - \mu_{Ta}$  (which sets the amount of Bi anti-sites) and  $\mu_O$  (which sets the amount of O vacancies). Fig. 3 shows the hole carrier concentration under different growth conditions (as characterized by these sets of variables). The difference  $\mu_K - \mu_{Ba}$  (reported along the y-axis) goes from a K-poor/Ba-rich to a K-rich/Ba-poor environment; while the difference  $\mu_{Bi} - \mu_{Ta}$  (reported along the x-axis) goes from a Bi-poor/Ta-rich to a Bi-rich/Ta-poor environment. Three different plots corresponding to different  $O_2$  environments are reported. In the low  $\mu_O$  region and for reducing conditions,  $Vac_O^{2+}$  has the dominant role in compensating p-type doping, and it is impossible to get a carrier concentration greater than  $10^{10} \text{ cm}^{-3}$  leading indeed to an insulating material in all conditions. As  $\mu_O$  increases (*i.e.* moving towards oxidizing conditions), regions of higher hole carrier concentration appear but only with high  $\mu_{Bi}$  and  $\mu_K$ . High  $\mu_{Bi}$  is needed to avoid a too high concentration of compensating defects (Ta on Bi antisites) and high  $\mu_K$  is needed to bring enough shallow acceptor defects. The highest hole carrier concentration of  $10^{16} \text{ cm}^{-3}$  can be obtained only in a narrow range of process conditions. This carrier concentration is still low and in qualitative agreement with the low carrier concentration ( $10^{14} \text{ cm}^{-3}$ ) measured experimentally. In the best conditions, the conductivity in K-doped  $Ba_2BiTaO_6$  is clearly limited by charge compensation from donor defects ( $Vac_O^{2+}$ ,  $Ta_{Bi}^{2+}$ ).

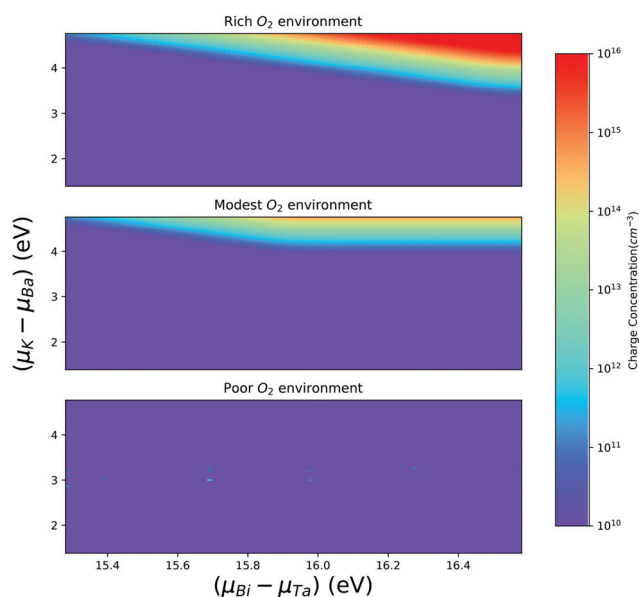


Fig. 3 Charge concentration under different growth conditions.

Table 1 Detailed defect concentrations at the most favorable chemical potentials for p-type doping, where the equilibrium Fermi level  $E_f = 0.2 \text{ eV}$ . The chemical potentials correspond to O, K, Bi rich and Ta, Ba poor environment

Defect	Charge	Defect concentration ( $\text{cm}^{-3}$ )
$Vac_{Ba}$	-2	0
$Vac_{Bi}$	-3	0
$Vac_O$	2	$7.15 \times 10^{21}$
$Bi_{Ta}$	0	$2.87 \times 10^{15}$
$Bi_{Ta}^i$	1	$4.25 \times 10^{14}$
$Ta_{Bi}$	2	$1.34 \times 10^{21}$
$Ta_{Bi}^i$	3	$2.43 \times 10^{20}$
$K_{Ba}$	-1	$1.77 \times 10^{22}$

The detailed free charge concentrations provided by the dominant defect is given in Table 1 for the region of favorable p-type behavior. The net free holes created by  $K_{\text{Ba}}$ ,  $\text{Bi}_{\text{Ta}}$ , and  $\text{Vac}_{\text{Ba}}$  is compensated by the donors  $\text{Vac}_{\text{O}}$  and  $\text{Ta}_{\text{Bi}}$ .

## Discussion

Our analysis shows that even using the most favorable growth conditions and a shallow acceptor such as K, the hole carrier concentration is still very limited in  $\text{Ba}_2\text{BiTaO}_6$ . This directly comes from two hole-killing defects: the O vacancy and the Ta on Bi anti-site.

On a general note, our work shows that quaternary compounds can lead to intrinsic challenges in terms of carrier engineering. Indeed, while the compensation by O vacancy is very common in oxides and has been reported for many binaries,<sup>38,39</sup> we observe here that an additional hole-killing defect has to be taken into account: the Ta on Bi anti-site. For multi-element materials such as quaternaries, the possibility for these additional hole-killer to be limiting the carrier concentration increases as well.

Our work indicates that high conductivity  $\text{Ba}_2\text{BiTaO}_6$  if it could ever be achieved would be obtained by working within high  $\mu_{\text{O}}$  conditions (oxidizing conditions) as well as high  $\mu_{\text{Bi}}$  conditions (Bi excess). We would like to point out that our work assumes equilibrium conditions and that working out-of-equilibrium could be a way to push out of the limiting chemical potential boundaries and increase the carrier concentration. In any case,  $\text{Ba}_2\text{BiTaO}_6$  appears to be a material which is very difficult to dope to high carrier concentrations.

One possibility to go forward is to keep the Bi in the perovskite structure and replace Ta to lower the anti-site  $\text{Ta}_{\text{Bi}}^{2+}$  defects.  $\text{Ba}_2\text{BiSbO}_6$ <sup>40–43</sup> retains the dispersion in the top of the valence band which maintains a relatively low hole effective mass ( $0.91 m_e$ ),<sup>44</sup> with a smaller yet still high enough band gap (3 eV). This makes it another interesting p-type TCO candidate. Unfortunately, our defect computations (carried out only at PBE level, through correcting the band gap with HSE)<sup>45,46</sup> show that intrinsic donor defects  $\text{Vac}_{\text{O}}^{2+}$  and  $\text{Sb}_{\text{Bi}}^{2+}$  in K-doped  $\text{Ba}_2\text{BiSbO}_6$  (more details in ESI†) are still the major defects that compensate the conductive holes. We therefore expect similar doping issues for  $\text{Ba}_2\text{BiSbO}_6$ .

Our calculations considering a stoichiometric  $\text{Ba}_2\text{BiTaO}_6$  suggest that moving towards higher Bi content mixed oxides such as  $\text{Ba}_2\text{Bi}_{1+x}\text{Ta}_{1-x}\text{O}_6$  (that would also be doped by K) could be a way forward to increase carrier concentration. We note that such solid solutions have been synthesized previously.<sup>47</sup> Increasing the Bi content will increase  $\mu_{\text{Bi}}$  and lower the compensation from Ta on Bi anti-site defects. This increase in Bi content while favorable for conductivity could however decrease transparency. Our computations indicate that a  $\text{Ba}_2\text{Bi}_{1.125}\text{Ta}_{0.875}\text{O}_6$  with 0.125% extra Bi introduces a state within the band gap and causes a reduction in the band gap to 2.54 eV, which might affect the light absorption of the material (see ESI†). This is not surprising in view of the lower band gap of  $\text{BaBiO}_3$ . A compromise might have to be found

with the amount of Bi excess as it could lead to high conductivity but lower the transparency.

## Conclusions

Using first-principles computations we have studied the defects of  $\text{Ba}_2\text{BiTaO}_6$  doped with K which is a possible high mobility p-type transparent oxide. Two dominant intrinsic donor defects  $\text{Vac}_{\text{O}}^{2+}$  and  $\text{Ta}_{\text{Bi}}^{2+}$  compensate the holes provided from the extrinsic dopant ( $\text{K}_{\text{Ba}}^{1-}$ ). The best hole carrier concentration can be achieved by synthesis conditions favoring a high chemical potential of O, K, and Bi. Our computed highest hole equilibrium carrier concentration is found to be around  $10^{16} \text{ cm}^{-3}$  which is still low for practical applications. We suggest that exploring the mixed oxide  $\text{Ba}_2\text{Bi}_{1+x}\text{Ta}_{1-x}\text{O}_6$  could offer an avenue towards increasing carrier concentration beyond these limits.

## Conflicts of interest

There are no conflicts to declare.

## Acknowledgements

The authors thank J. B. Varley and J. Suntivich for useful discussions. D. D. was financed by the Conseil de L'Action Internationale (CAI) through a doctorate grant "Coopération au Développement". G.-M. R. is grateful to the F. R. S.-FNRS (Belgium) for financial support. We acknowledge access to various computational resources: the Tier-1 supercomputer of the Fédération Wallonie-Bruxelles funded by the Walloon Region (grant agreement no. 1117545), and all the facilities provided by the Université catholique de Louvain (CISM/UCL) and by the Consortium des Equipements de Calcul Intensif en Fédération Wallonie-Bruxelles (CÉCI).

## References

- 1 T. Minami, New n-type transparent conducting oxides, *MRS Bull.*, 2000, **25**, 38–44.
- 2 S. C. Dixon, D. O. Scanlon, C. J. Carmalt and I. P. Parkin, n-type doped transparent conducting binary oxides: an overview, *J. Mater. Chem. C*, 2016, **4**, 6946–6961.
- 3 H. Kawazoe, H. Yanagi, K. Ueda and H. Hosono, Transparent p-type conducting oxides: design and fabrication of p-n heterojunctions, *MRS Bull.*, 2000, **25**, 28–36.
- 4 K. Ellmer, Past achievements and future challenges in the development of optically transparent electrodes, *Nat. Photonics*, 2012, **6**, 809–817.
- 5 H. Ohta and H. Hosono, Transparent oxide optoelectronics, *Mater. Today*, 2004, **3**, 42–51.
- 6 H. Ohta, M. Hirano, K. Nakahara, H. Maruta, T. Tanabe, M. Kamiya, T. Kamiya and H. Hosono, Fabrication and photoresponse of a pn-heterojunction diode composed of transparent oxide semiconductors, p-NiO and n-ZnO, *Appl. Phys. Lett.*, 2003, **83**, 1029–1031.

- 7 M. Izaki, T. Shinagawa, K. T. Mizuno, Y. Ida, M. Inaba and A. Tasaka, Electrochemically constructed p-Cu<sub>2</sub>O/n-ZnO heterojunction diode for photovoltaic device, *J. Phys. D: Appl. Phys.*, 2007, **40**, 3326–3329.
- 8 D. C. Look, T. C. Droubay and S. A. Chambers, Stable highly conductive ZnO via reduction of Zn vacancies, *Appl. Phys. Lett.*, 2012, **101**, 1–4.
- 9 H. Agura, A. Suzuki, T. Matsushita, T. Aoki and M. Okuda, Low resistivity transparent conducting Al-doped ZnO films prepared by pulsed laser deposition, *Thin Solid Films*, 2003, **445**, 263–267.
- 10 E. Fortunato, R. Barros, P. Barquinha, V. Figueiredo, S. H. K. Park, C. S. Hwang and R. Martins, Transparent p-type SnOx thin film transistors produced by reactive rf magnetron sputtering followed by low temperature annealing, *Appl. Phys. Lett.*, 2010, **97**, 1–4.
- 11 Y. Ogo, H. Hiramatsu, K. Nomura, H. Yanagi, T. Kamiya, M. Hirano and H. Hosono, P-channel thin-film transistor using p-type oxide semiconductor, SnO, *Appl. Phys. Lett.*, 2008, **93**, 1–4.
- 12 H. Peelaers, E. Kioupakis and C. G. Van de Walle, Free-carrier absorption in transparent conducting oxides: Phonon and impurity scattering in SnO<sub>2</sub>, *Phys. Rev. B: Condens. Matter Mater. Phys.*, 2015, **92**, 235201.
- 13 G. Hautier, A. Miglio, G. Ceder, G.-M. Rignanese and X. Gonze, Identification and design principles of low hole effective mass p-type transparent conducting oxides, *Nat. Commun.*, 2013, **4**, 2292.
- 14 G. Hautier, A. Miglio, D. Waroquiers, G.-m. Rignanese and X. Gonze, How does chemistry influence electron effective mass How does chemistry influence electron effective mass in oxides? A high-throughput computational analysis, *Chem. Mater.*, 2014, **26**, 5447–5458.
- 15 H. Kawazoe, M. Yasukawa, H. Hyodo, M. Kurita, H. Yanagi and H. Hosono, P-type electrical conduction in transparent thin films of CuAlO<sub>2</sub>, *Nature*, 1997, **38**, 939–942.
- 16 Y. Ogo, H. Hiramatsu, K. Nomura, H. Yanagi, T. Kamiya, M. Kimura, M. Hirano and H. Hosono, Tin monoxide as an s-orbital-based p-type oxide semiconductor: Electronic structures and TFT application, *Phys. Status Solidi A*, 2009, **206**, 2187–2191.
- 17 V.-A. Ha, F. Ricci, G.-M. Rignanese and G. Hautier, Structural design principles for low hole effective mass s-orbital-based p-type oxides, *J. Mater. Chem. C*, 2017, **5**, 5772.
- 18 D. O. Scanlon, J. Buckeridge, C. R. A. Catlow and G. W. Watson, Understanding doping anomalies in degenerate p-type semiconductor LaCuOSe, *J. Mater. Chem. C*, 2014, **2**, 3429–3438.
- 19 K. Ueda, S. Inoue, S. Hirose, H. Kawazoe and H. Hosono, Transparent p-type semiconductor: LaCuOS layered oxysulfide, *Appl. Phys. Lett.*, 2000, **77**, 2701–2703.
- 20 H. Hiramatsu, K. Ueda, H. Ohta, M. Hirano, T. Kamiya and H. Hosono, Degenerate p-type conductivity in wide-gap LaCuOS<sub>1-x</sub>Se<sub>x</sub> (x = 0–1) epitaxial films, *Appl. Phys. Lett.*, 2003, **82**, 1048–1050.
- 21 D. O. Scanlon and G. W. Watson, (Cu<sub>2</sub>S<sub>2</sub>)(Sr<sub>3</sub>Sc<sub>2</sub>O<sub>5</sub>)-A layered, direct band gap, p-type transparent conducting oxychalcogenide: A theoretical analysis, *Chem. Mater.*, 2009, **21**, 5435–5442.
- 22 G. Brunin, F. Ricci, V.-A. Ha, G.-M. Rignanese and G. Hautier, Transparent conducting materials discovery using high-throughput computing, *npj Comput. Mater.*, 2019, **5**, 1–12.
- 23 A. Bhatia, T. Nilgianskul, A. Miglio, J. Sun, H. J. Kim, K. H. Kim, S. Chen, G.-m. Rignanese, X. Gonze and J. Suntivich, High-mobility Bismuth-based transparent p-type oxide from high-throughput material screening, *Chem. Mater.*, 2016, 26–30.
- 24 H. Hiramatsu, H. Yanagi, T. Kamiya, K. Ueda, M. Hirano and H. Hosono, Crystal structures, optoelectronic properties, and electronic structures of layered oxychalcogenides MCuOCh (M = Bi, La; Ch = S, Se, Te): Effects of electronic configurations of M<sup>3+</sup> ions, *Chem. Mater.*, 2008, **20**, 326–334.
- 25 P. E. Blöchl, Projector augmented-wave method, *Phys. Rev. B: Condens. Matter Mater. Phys.*, 1994, **50**, 17953–17979.
- 26 G. Kresse and J. Furthmüller, Efficient iterative schemes for *ab initio* total-energy calculations using a plane-wave basis set, *Phys. Rev. B: Condens. Matter Mater. Phys.*, 1996, **54**, 11169–11186.
- 27 G. Kresse and J. Furthmüller, Efficiency of *ab-initio* total energy calculations for metals and semiconductors using a plane-wave basis set, *Comput. Mater. Sci.*, 1996, **6**, 15–50.
- 28 C. Freysoldt, B. Grabowski, T. Hickel, J. Neugebauer, G. Kresse, A. Janotti and C. G. Van de Walle, First-principles calculations for point defects in solids, *Rev. Mod. Phys.*, 2014, **86**, 253–305.
- 29 D. Broberg, B. Medasani, N. E. R. Zimmermann, G. Yu, A. Canning, M. Haranczyk, M. Asta and G. Hautier, PyCDT: A Python toolkit for modeling point defects in semiconductors, *Comput. Phys. Commun.*, 2018, **226**, 165–179.
- 30 J. Perdew, K. Burke and M. Ernzerhof, Generalized Gradient Approximation Made Simple, *Phys. Rev. Lett.*, 1996, **77**, 3865–3868.
- 31 J. Heyd, G. E. Scuseria and M. Ernzerhof, Hybrid functionals based on a screened Coulomb potential, *J. Chem. Phys.*, 2003, **118**, 8207–8215.
- 32 J. L. Lyons and C. G. Van De Walle, Computationally predicted energies and properties of defects in GaN, *npj Comput. Mater.*, 2017, **3**, 12–21.
- 33 S. B. Zhang and J. E. Northrup, Chemical Potential Dependence of Defect Formation Energies in GaAs: Application to Ga Self-Diffusion, *Phys. Rev. Lett.*, 1991, **67**, 2339–2342.
- 34 H. P. Komsa, T. T. Rantala and A. Pasquarello, Finite-size supercell correction schemes for charged defect calculations, *Phys. Rev. B: Condens. Matter Mater. Phys.*, 2012, **86**, 045112.
- 35 C. Freysoldt and C. G. Van de Walle, Electrostatic interactions between charged defects in supercells, *Phys. Status Solidi B*, 2011, **1076**, 1067–1076.
- 36 Y. Kumagai and F. Oba, Electrostatics-based finite-size corrections for first-principles point defect calculations, *Phys. Rev. B: Condens. Matter Mater. Phys.*, 2014, **89**, 1–15.
- 37 B. A. Baumert, Barium potassium bismuth oxide: A review, *J. Supercond.*, 1995, **8**, 175–181.
- 38 J. Robertson and S. J. Clark, Limits to doping in oxides, *Phys. Rev. B: Condens. Matter Mater. Phys.*, 2011, **83**(7), 075205.
- 39 D. O. Scanlon and G. W. Watson, On the possibility of p-type SnO<sub>2</sub>, *J. Mater. Chem.*, 2012, **22**, 25236–25245.
- 40 C. F. Xing, J. Bao, Y. F. Sun, J. J. Sun and H. T. Wu, Ba<sub>2</sub>BiSbO<sub>6</sub>: A novel microwave dielectric ceramic with monoclinic structure, *J. Alloys Compd.*, 2019, **782**, 754–760.

- 41 M. C. Castro, C. W. D. A. Paschoal, F. C. Snyder and M. W. Lufaso, Relaxations in  $\text{Ba}_2\text{BiSbO}_6$  double complex perovskite ceramics, *J. Appl. Phys.*, 2008, **104**, 104114.
- 42 W. Fu, A neutron powder diffraction study on  $\text{BaBi}_{0.5}\text{Sb}_{0.5}\text{O}_3$ , *Solid State Commun.*, 2000, **116**, 461–464.
- 43 B. Kennedy, C. Howard, K. Knight, Z. Z. Ming and Z. Q. Di, Structures and phase transitions in the ordered double perovskites  $\text{Ba}_2\text{Bi(III)Bi(V)O}_6$  and  $\text{Ba}_2\text{Bi(III)Sb(V)O}_6$ , *Acta Crystallogr., Sect. B: Struct. Sci.*, 2006, **62**, 537–546.
- 44 F. Ricci, W. Chen, U. Aydemir, G. J. rey Snyder, G.-M. Rignanese, A. Jain and G. Hautier, An *ab initio* electronic transport database for inorganic materials, *Sci. Data*, 2017, **4**, 170085.
- 45 A. Alkauskas, P. Broqvist and A. Pasquarello, Defect energy levels in density functional calculations: Alignment and band gap problem, *Phys. Rev. Lett.*, 2008, **101**, 046405.
- 46 A. Alkauskas, P. Broqvist and A. Pasquarello, Defect levels through hybrid density functionals: Insights and applications, *Phys. Status Solidi B*, 2011, **248**, 775–789.
- 47 H. Wang, C.-h. Wang, G. Li, T. Jin, F. Liao and J. Lin, Synthesis, Structure, and Characterization of the Series  $\text{BaBi}_{(1-x)}\text{Ta}_x\text{O}_3$  ( $0 < x < 0.5$ ), *J. Am. Chem. Soc.*, 2010, **3**, 5262–5270.